Macromolecules

ARTICLE

pubs.acs.org/Macromolecules

Random Scission of Polymers: Numerical Simulations, and Experiments on Hyaluronan Hydrolysis

Aernout A. Martens,[*,†,‡] Nicolaas A. M. Besseling,[*,†] Saskia Rueb,[‡] Ernst J. R. Sudhölter,[†] Herman P. Spaink,[‡] and Louis C. P. M. de Smet[†]

[†]Department of Chemical Engineering, Delft University of Technology, Julianalaan 136, 2628 BL Delft, The Netherlands

[‡]Institute of Biology, Leiden University, Leiden, The Netherlands

Supporting Information

ABSTRACT: We present a study of the random scission process of polymers, in which numerical simulations are combined with experimental investigations into the acid hydrolysis of the polysaccharide hyaluronan (HA), in particular at pH 1.1 and 50 °C. As input for the simulations, an initial molecular weight distribution ($MD_{(0)}$) and the hydrolysis rate constant (k_h) are needed. The first was obtained using agarose gel electrophoresis followed by densitometric analyses, by which we determined the evolution of the full molar-mass distribution during hydrolysis. The rate constant was experimentally obtained by two independent techniques. Kinetic plots were obtained from both the number- and the weight-average molar mass (M_n and M_w, respectively), converted to degrees of polymerization (N_n and N_w, respectively), and from these, k_h values for HA hydrolysis were derived. For confirmation, k_h was also determined from the evolution of the concentration of reducing chain ends. Experimentally determined k_h values were used as input for the model, and the evolution of MD during hydrolysis was simulated for various hypothetical $MD_{(0)}$ functions as well as for an experimentally determined $MD_{(0)}$ curve. Agreement between experimental and simulated results demonstrated consistency of the model and indicates that acid hydrolysis of hyaluronan can indeed be considered a random scission process. We show that for cases where the initial molar mass distribution is not of the Kuhn-type—which is often the case—the value for the k_h determined from the evolution of M_n is more accurate than that obtained from M_w.

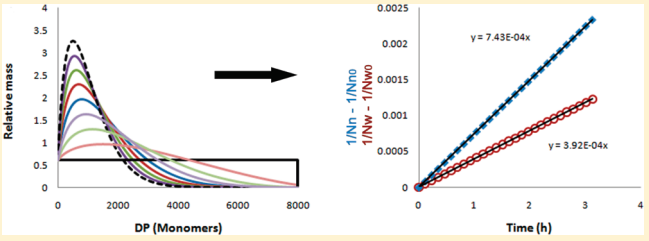

1. INTRODUCTION

Random scission of polymers and the determination of scission rate constants have been described as early as 1930 by Kuhn,[1] who studied the degradation of natural polymers (since at that time there were almost no synthetic polymers). Using a population balance model,[1] he found that extensive degradation of linear polymers by random scission had to lead to a type of self-preserving distribution, now often called a Kuhn distribution. This Kuhn distribution is in fact identical to the distribution generated upon random formation of polymers, as derived by Flory.[2] Once established, a Kuhn distribution remains preserved upon further degradation, while shifting to lower molecular masses. When starting from a theoretical monodisperse polymer, exact solutions can be found for (a) the convergence to a shifting Kuhn distribution and (b) the number and weight-average molecular masses (M_n and M_w) as a function of time.[3,4]

However, when starting from an arbitrary molecular mass distribution (MD), e.g., as found for natural polymers, degradation and convergence toward a Kuhn distribution can only be simulated numerically,[5,6] which has become possible with the appearance of computers. We combined numerical modeling with degradation experiments of a polydisperse polymeric starting material as may occur in practical situations. Moreover, we addressed the implications for the determination of scission rate constants when the initial MD is not of the Kuhn type. The polymer of our choice, hyaluronan, is particularly interesting because of its many molecular mass-dependent biological functions and biomedical applications.[7]

Hyaluronan (HA),[8] also called hyaluronic acid or hyaluronate, is a linear glucosaminoglycan (GAG) that consists of repeating disaccharide units. The disaccharide units consist of *N*-acetyl-D-glucosamine (GlcNAc) and D-glucuronic acid (GlcA), linked by a β(1→4)-glycosidic bond, while the disaccharides are linked by β(1→3)-bonds. GlcA possesses a carboxylic acid group and is therefore negatively charged at neutral pH and is protonated at low pH. This ubiquitous polymer is found in the extracellular matrix and on the cell surfaces of almost every vertebrate tissue, serving both structural and signaling functions. HA plays an important role in a large variety of biological processes, for instance involving cell locomotion processes[8] underlying leukocyte

Received: January 4, 2011
Revised: March 16, 2011
Published: March 28, 2011

homing,[9] cancer metastasis,[7,9] angiogenesis,[7] and embryonic development.[7,10] Because of its interesting physiochemical properties and biocompatibility,[11] HA has been used in a large variety of biomedical applications, including ophthalmic surgery, osteoarthritis treatment and for facilitating the healing and regeneration of surgical wounds.[12,13] HA is also used as an ingredient in cosmetics and there is an increasing number of studies on HA applications in the area of cancer treatment and drug delivery. The molecular mass (M) of HA is a determining factor for its function,[7] not just because of M-dependent physical properties, but mainly because different values for M are recognized as different biological signals leading to seriously different biological effects.[7]

In the light of the M-dependent HA properties,[7] combined with the wide and increasing use of HA in different biomedical applications,[12,13] control over the HA size is very important, both in terms of average M, as well as in terms of the complete molecular mass distribution (MD).[14] Different methods are available to obtain HA of different length and MD, including enzymatic[15,16] or bacterial[17] synthesis, and chemical,[14] enzymatic[14] or ultrasonic[14,18] degradation of synthesized or biologically derived[17] HA. While for research purposes expensive samples of highly defined HA are available, larger amounts at lower costs are needed for (bio)medical and cosmetics applications.

An interesting, cost-effective method to reduce the length of HA is the hydrolysis of HA in acidic solutions.[14,19] As reported by others,[19] and confirmed by our present investigations (*vide infra*), this degradation process occurs by random scission of the polymer chains. In such a random scission process, the probability of a monomer−monomer bond to be cleaved is equal for all bonds within a chain. Random scission of any linear polymer eventually leads to a typical Kuhn distribution,[1] for which, the ratio between the weight-average molecular mass (M_w) and the number-average molecular mass (M_n), the polydispersity index, M_w/M_n equals 2.[1] If the initial MD, $MD_{(0)}$, is already a Kuhn distribution, the form of the distribution does not change during the random scission process, and consequently the M_w/M_n remains 2 throughout the process. However, when starting from an arbitrary MD, the MD converges toward a Kuhn distribution during random scission and M_w/M_n will be a function of degradation time.[1]

In carbohydrate chemistry, the most common way to determine k_h is based on analysis of experimentally obtained MDs at different degradation times. In more detail, M_w is determined from the MD data. Subsequently, k_h is derived from the resulting $M_{w(t)}$ data according to what is sometimes called the Ekenstam relationship:[5]

$$\frac{1}{N_{w(t)}} - \frac{1}{N_{w(0)}} = \frac{1}{2}k_h t \text{ or } \frac{1}{M_{w(t)}} - \frac{1}{M_{w(0)}} = \frac{k_h t}{2m} = \frac{1}{2}k'_h t \quad (1)$$

Here, N_w is the weight-average degree of polymerization: "number of monomers in a polymer chain". For HA we take a monomer to correspond to a disaccharide. M_w is the weight-average molecular mass, and m is the molecular mass of a monomer. k_h is *twice* the slope in the (linear) $1/M_{w(t)} - 1/M_{w(0)}$ vs time plot.[2,5,19,20] The factor of 2 in the slopes results from the $M_w/M_n = 2$ ratio for Kuhn distributions.[1,20] It is, however, equally possible to determine k_h from $M_{n(t)}$, because k_h is exactly the slope in the $1/M_{n(t)} - 1/M_{n(0)}$ vs time plot:

$$\frac{1}{N_{n(t)}} - \frac{1}{N_{n(0)}} = k_h t \text{ or } \frac{1}{M_{n(t)}} - \frac{1}{M_{n(0)}} = \frac{k_h t}{m} = k'_h t \quad (2)$$

In order to predict the evolution of the MD under hydrolysis conditions, a model is required. To this end we built a numerical population balance model to simulate the MD evolution during random scission, and compared the results to experimental data. In particular, we are interested in comparing the two approaches for calculating k_h from $MD_{(t)}$: either through the Ekenstam relationship for the evolution of M_w or N_w, or through the alternative relationship for M_n or N_n, in effect using either eq 1 or eq 2.

To acquire experimental MDs and k_h, for use as input for the presented model, and for later comparison to model results, we took HA samples at different times during degradation at 50 °C and pH 1.1. Subsequently we subjected these samples to agarose gel electrophoresis for MD determination[21] and subsequent calculation of k_h. We also determined k_h independently using the dinitrosalicylic acid (DNS) reducing sugar assay.[22] When a glucoside bond is broken, a reducing end is formed. Since every bond cleavage leads to one reducing end, we can determine k_h from the increase in reducing ends with increasing sampling time and see whether it is consistent with the value for k_h determined from MD evolution.

2. MODEL FOR RANDOM SCISSION OF A LINEAR POLYMER

2.1. Assumptions and Model Input. During a random scission process of a linear polymer, the probability of a monomer−monomer bond to be cleaved is equal for all bonds. Since the β (1→4) GlcNAc-GlcA bond is much more prone to acid hydrolysis than the β (1→3) GlcA-GlcNAc glycosidic bond,[23] we do not regard the monosaccharides, but the GlcA-GlcNAc disaccharide units as the monomers that constitute the chain. As input for the model we need the initial MD ($MD_{(0)}$) and the hydrolysis rate constant (k_h) that expresses how many bonds are broken per number of bonds present per unit time.

Because the presented model is applicable to random degradation of linear polymers in general, evaluating possible differences in k_h depending on calculation method, using a hypothetical non-Kuhn $MD_{(0)}$ as input will be of general interest. However, to see how the model holds up in practice, in this case for HA, we will also explore experimentally determined initial MDs as input.

Such input was acquired from an experiment in which HA was degraded at 50 °C in the presence of 0.1 M HCl. Full molecular weight distributions were determined at different stages of the process by means of gel electrophoresis and subsequent densitometric analysis. From these MDs, both $N_{w(t)}$ and $N_{n(t)}$ were readily deduced. Subsequently, a k_h was determined both from $N_{w(t)}$ and from $N_{n(t)}$, using eq 1 and 2, respectively. Using $MD_{(0)}$ and either k_h as input, $MD_{(t)}$ could be simulated yielding simulated $N_{w(t)}$ and $N_{n(t)}$ with, in the end, each their own simulated k_h. These calculations allowed us to ascertain whether the procedure is internally consistent, and to analyze the differences between k_h determined experimentally either from the Ekenstam relation for N_w, or the alternative (N_n-based) relation.

2.2. Model Derivation and Description. To evaluate the procedures for obtaining the value for k_h as described above, we performed numerical simulations of the random degradation process as schematically represented in Figure 1. It is assumed that the GlcNAc−GlcA glycoside bonds connecting the disaccharide monomers of the hyaluronan chains degrade according

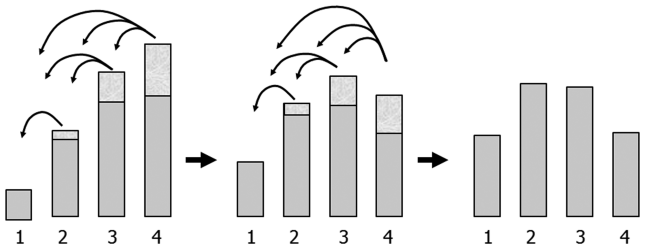

Figure 1. Scheme of the polymer degradation model, for an MD limited to monomers, dimers, trimers and tetramers (indicated by the numbers 1−4). On the left-hand side, we see the initial distribution, in the middle the distribution after one time step, and on the right-hand side the distribution after two time steps. The boxed top sections of the bars are the masses removed from each fraction during the next time step. These masses are distributed over fractions of lower molecular mass as indicated by the curved arrows. Consequently, each fraction can only gain mass from fractions of higher molecular mass. The amount of mass removed from a fraction (size of top box in scheme) is proportional to the number of bonds per molecule and the total mass in the fraction. For clarity, this representation only covers 4 populations and 2 time steps, hydrolyzing 10% of all bonds in each step, while the actual model covers 8000 populations and 27 time steps hydrolyzing less than 0.01% of all bonds per time step.

to first-order kinetics:

$$\frac{dc_b}{dt} = -k_h c_b \tag{3}$$

where c_b is the concentration of GlcNAc−GlcA glycoside bonds. Hence the number of bonds that are degraded per unit volume during a small time interval Δt is

$$\Delta c_b = -\Delta t k_h c_b \tag{4}$$

This holds as well for the degradation of bonds in a separate fraction of chains consisting of N disaccharide units, and $N-1$ GlcNAc−GlcA glucoside bonds per chain

$$\Delta_s c_{b,N} = -\Delta t k_h c_{b,N} \tag{5}$$

where $c_{b,N}$ is the concentration of bonds that belong to N-mers before the time step, and $\Delta_s c_{b,N}$ is the contribution to the change of c_b due to scissions in N-mers during the time step. Please note that $\Delta_s c_{b,N}$ has to be distinguished from $\Delta_l c_{b,N}$, which is the loss of the concentration of bonds in N-mers due to scission within these N-mers, since one breaking bond in an N-mer removes the entire chain from the N-mer fraction. Furthermore, we define, $c_{m,N} = Nc_N$ as the concentration of monomer units (disaccharides) that belong to N-mers, effectively representing the mass in the N-mer fraction. Obviously, $c_{m,N} = c_N N$, $c_{b,N} = c_N(N-1)$ (when no closed rings are present), and $c_{b,N}/c_{m,N} = (N-1)/N$. Furthermore, $\Delta_l c_{m,N}$ and $\Delta_l c_N$ represent the loss of monomers, and the loss of chains suffered by the N-fraction, due to chains ceasing to be N-mers because of scissions occurring during a time step Δt.

Provided that the number of bonds that are broken in a single chain during a time step is never larger than 1 (either 0 or 1), $\Delta_l c_N$, the contribution to the change of the concentration of N-mers due to chains ceasing to be N -mers, is equal to $\Delta_s c_{b,N}$:

$$\Delta_l c_N = \Delta_s c_{b,N} = -\Delta t k_h c_{b,N} \tag{6}$$

Hence, the change of the concentration of monomers present in N-mers is

$$\Delta_l c_{m,N} = \Delta_l c_N N = \Delta_s c_{b,N} N = -\Delta t k_h c_{b,N} N \tag{7}$$

and the change of the concentration of bonds present in N-mers is

$$\Delta_l c_{b,N} = \Delta_l c_N (N-1) = \Delta_s c_{b,N}(N-1) = -\Delta t k_h c_{b,N}(N-1) \tag{8}$$

This holds if the time step is made sufficiently small. The average number of bonds breaking in a single N-mer is $\Delta t k_h N$ and should be <1. Typical values that we use in our simulations are as follows: $k_h = 7.45 \times 10^{-4}$ (h^{-1}), $\Delta t = 0.12$ (h) and the longest chain in the model is $N = 8000$ monomers, so for the longest chains, $\Delta t k_h N = 0.7 < 1$, and for shorter N, the value will be even smaller.

Breaking of a bond at position n within in an N'-mer yields two fragments of sizes n and $N' - n$. For random degradation all $N' - 1$ possible values of n, ranging from 1 to $N' - 1$, are equally probable, with probability $1/(N' - 1)$. Hence *the fragments* formed by scission of N'-mers are evenly distributed over all values of the degree of polymerization (DP) that are smaller than N'. Hence, breakup of N'-mers during a time step contributes to each fraction with $N < N'$ an amount $2\Delta_l c_{N'}/(N' - 1)$ to the chain concentration of N-mers, $2\Delta_l c_{N'} N/(N' - 1)$ to the monomer concentration present in N-mers, and $2\Delta_l c_{N'}(N-1)/(N' - 1)$ to the bond concentration present in N-mers. The factor of 2 is there because cutting a single chain once results in two fragments. The number of broken single chains per unit volume from an N'-mer population ($\Delta_l c_N$) gives twice that number of chain fragments to be distributed equally over the smaller-chain fractions. Hence the contribution to the concentration change of bonds in N-mers due to breaking of chains with a DP > N is given by

$$\Delta_g c_{m,N} = \sum_{N'=N+1}^{\infty} 2\Delta_l c_{N'} N/(N' - 1) \tag{9}$$

where in a practical simulation, a finite upper cutoff value for the DP has to be used. We used a cutoff value of 8000. For all measured and modeled input MDs (later in this paper), the polymer mass above 8000 was <0.5% of the total mass.

We simulate the evolution of MD by calculating the MD after a time step s from that before the time step as

$$c_{m,N,s} = c_{m,N,s-1} + \Delta_l c_{m,N,s} + \Delta_g c_{m,N,s} \tag{10}$$

where $c_{m,N,s}$ is the concentration of disaccharide monomers present in N-mers after time step s, $\Delta_l c_{m,N,s} (\leq 0)$ represents the loss of monomers from the N-fraction, and $\Delta_g c_{m,N,s} (\geq 0)$ represents the gain of monomers present in the N-fraction.

In essence, the sum over all DP values of the weight distribution of the molecular weight (or DP) represents the total HA mass present. During each time step, mass (disaccharide monomers) is moved from higher M fractions to lower M fractions, but the total amount of monomers stays the same. Parts a and d of Figure 2 are examples of such a simulated MD development. Because of computational limitations, simulations were limited to 27 iterations, yielding 28 MDs including $t = 0$.

3. RESULTS AND DISCUSSION

3.1. Simulations of Degradation of Hypothetical Initial Distributions. We simulated $MD_{(s)}$, $N_{w(t)}$, and $N_{n(t)}$ for various hypothetical $MD_{(0)}$ input. From these simulations we plot $1/N_{w(0)} - 1/N_{w(t)}$ and $1/N_{n(0)} - 1/N_{n(t)}$ vs time, and derive $k_h/2$ and k_h from their slopes, respectively. The input value of k_h was 7.45×10^{-4} (h^{-1}), as was determined experimentally for

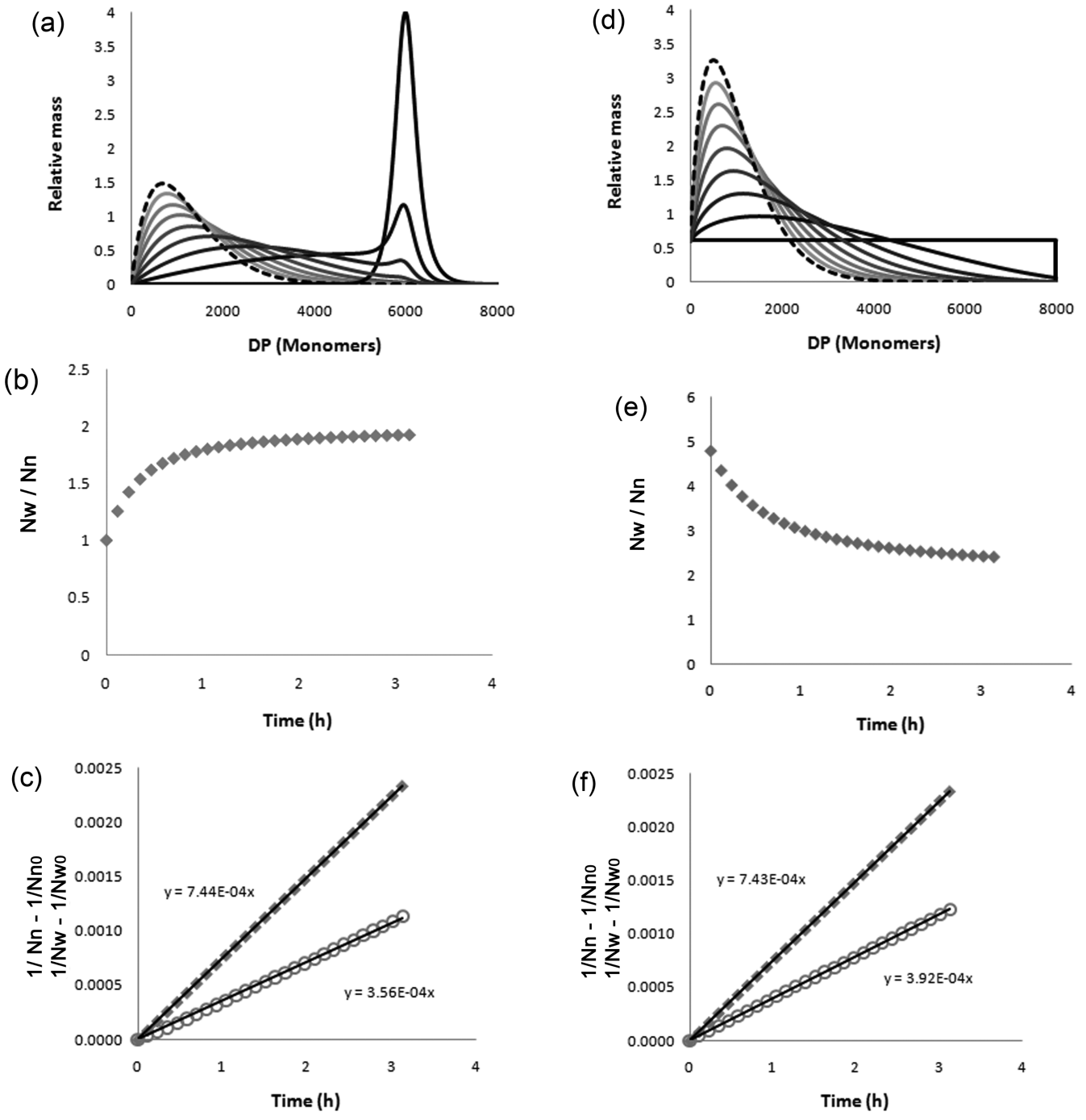

Figure 2. Numerical simulation of the polymer MD evolution during random scission (k_h =7.45 × 10^{-4} (h^{-1}). (a) Degradation of a narrow peak distribution (black solid line with peak at DP = 6000) with relative mass on the ordinate and degree of polymerization (DP) on the abscissa. The gray lines depict every second iteration, as time progresses the lines become lighter in color until iteration 16 (black dotted line) corresponding to time =1.9 h. The full simulation was 27 iterations corresponding to 3.1 h, of which the remaining MDs are not depicted in part a, but they are included in part b, showing N_w/N_n ratio development in time. (c) Kinetic plot for N_n and N_w showing: $1/N_{n(0)} - 1/N_{n(t)}$ as a function of time (solid rhombi) and $1/N_{w(0)} - 1/N_{w(t)}$ as a function of time (open circles). Parts d−f are analogous to parts a−c of Figure 2, respectively, the difference being that the $MD_{(0)}$ is a broad distribution instead of a narrow peak.

acid HA hydrolysis discussed later in this paper. When entering a Kuhn distribution as $MD_{(0)}$ (not shown), k_h calculated from N_w and N_n were both 7.43 × 10^{-4} (h^{-1}). This confirms the internal consistency of our model, because when degrading a Kuhn distribution, an analysis based on the Ekenstam relation for N_w, and the alternative in terms of N_n should both yield the same value for k_h, (which should obviously be the same as the input k_h). The minor deviation from the input is caused by numerical inaccuracy.

To evaluate the determination of k_h from N_w and from N_n in case of non-Kuhn distributed $MD_{(0)}$, we entered a narrow peak distribution (Figure 2a) and a highly polydisperse broad

dx.doi.org/10.1021/ma200009y |*Macromolecules* 2011, 44, 2559–2567

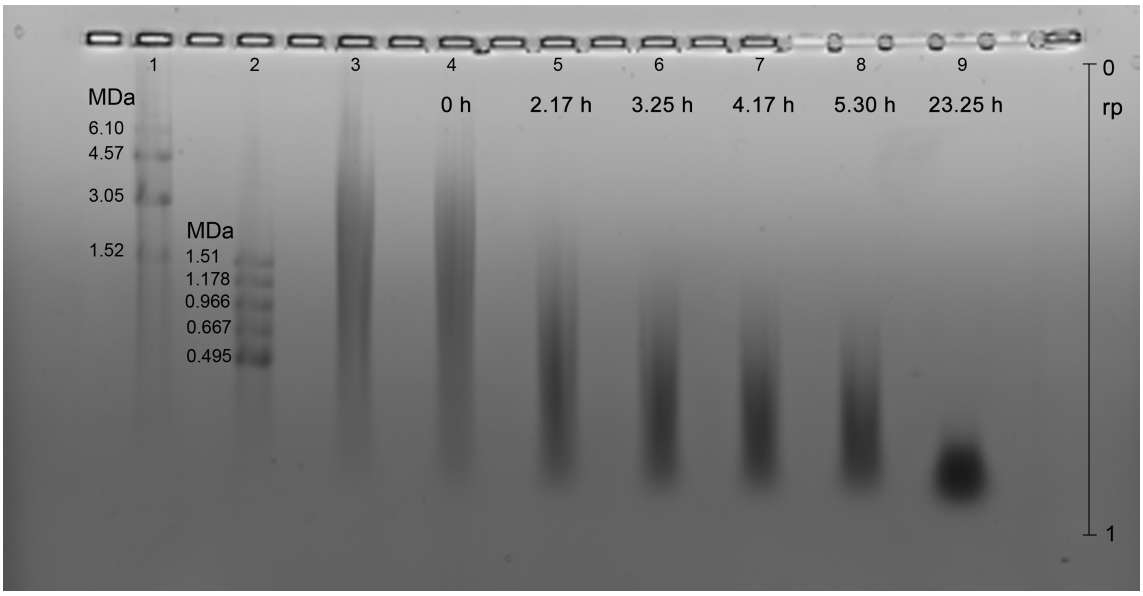

Figure 3. Densitometric image of an agarose gel after electrophoresis and staining of HA. Lanes 1 and 2: molecular mass markers in MDa. Lane 3: *S. zooepidemicus* HA source. Lane 4 HA as used in the degradation mix. Lanes 5−9 samples of the degrading HA in time corresponding to samples taken at 2.17, 3.25, 4.17, 5.30, and 23.25 h after mixing with acid and placement in an oven at 50 °C. On the right-hand side the relative position (rp) scale, used for densitometric readout, is given.

distribution (Figure 2d) as initial distributions and compared the k_h values resulting from calculations to the input k_h, and to each other.

Figure 2a shows the development of the MD during random scission starting from a peak distribution $MD_{(0)}$ (solid black line). The gray lines represent MDs every 2 time steps (of 0.12 h each), until time step 16 (dotted black line) at a simulated time of 1.9 h. The full simulation up to 27 time steps covered 3.1 h. As a function of time, the MDs converged toward a Kuhn MD, resembling a Kuhn MD the most in the end ($MD_{(27)}$), and $MD_{(16)}$ being the most Kuhn-like MD depicted in Figure 2a (dotted black line). This development is qualitatively the same as for other of random scission simulations,[5,6] showing that models like this can be applied to random degradation of any linear polymer, irrespective of the mechanism and rate by which random scission occurs. As a consequence of the convergence toward a Kuhn distribution, the N_w/N_n ratio in Figure 2b increases gradually from 1 (indicative of monodispersity) to 2 (indicative of a Kuhn distribution). We observe that for the full simulation starting with an $MD_{(0)}$ as in Figure 2a, the kinetic plots of $1/N_n$ and $1/N_w$ (Figure 2c) gave slopes corresponding to a k_h of 7.44×10^{-4} (h^{-1}) and 7.12×10^{-4} (h^{-1}), respectively. The N_n-derived k_h is practically the same as the input k_h whereas the N_w-derived k_h is 4% lower. The $1/N_w$ data show some deviation from linearity at the initial stages of degradation, originating from the fact that N_w/N_n is not yet equal to 2.

Figure 2d shows the development of the MD during random scission for a hypothetical polydisperse "block" distribution $MD_{(0)}$ (solid black line). The MD development is depicted as in Figure 2a, the gray lines reflecting MD development and the dotted black line the resulting $MD_{(16)}$ at t = 1.9 h. Figure 2e shows the corresponding N_w/N_n ratio slowly converging from 5, indicating large polydispersity, to 2, indicative of a Kuhn distribution. The N_n- and N_w-based kinetic plots (Figure 2f) yield $k_h = 7.43 \times 10^{-4}$ (h^{-1}) and $k_h = 7.84 \times 10^{-4}$ (h^{-1}), respectively. Again, it is observed that the N_n-derived k_h is practically the same as the input k_h, while the N_w-derived k_h deviates (5% higher this time).

The deviation becomes larger when k_h is calculated over shorter degradation times. For example, simulations like the one shown in Figure 2a for simulated times of 1 and 0.1 h (not shown) give deviations in N_w-derived k_h of −17% and −31%, respectively, while the N_n-derived k_h consistently remains 7.45×10^{-4} (h^{-1}) in both cases. This analysis shows that plotting $1/N_n$ to determine k_h from MD measurements works well, independently of the initial distribution $MD_{(0)}$, while an analysis based on N_w is only valid for MDs that are close to Kuhn MD.

3.2. HA Hydrolysis and MD Determination by Densitometry. To acquire experimental data for comparison to our numerical simulations, *Streptococcus zooepidemicus* HA was degraded at a measured pH of 1.1 and temperature of 50 °C. We studied the acid-catalyzed degradation of HA by taking samples from the acidic HA solution at different stages during degradation, and determining the MD in each sample. MDs were determined as basically described by Lee and Cowman,[21] by subsequent agarose gel electrophoresis, gel staining, and acquisition of a densitometric image (Figure 3), yielding optical density profiles, from which full MDs could be calculated (shown in Supporting Information). Samples were loaded in the slots at the top of the gel (Figure 3). During electrophoresis, small chains travel fast, ending up low on the gel close to a relative position on the gel (rp) of 1, while large chains travel slowly, ending up high on the gel (rp ∼0). Lanes 1 and 2 contain molecular mass markers that enable us to estimate the MDs as described in detail in the Supporting Information. Lane 3 contains the original *S. zooepidemicus* HA after careful dissolution. Lane 4 contains a slightly degraded and more polydisperse HA sample (treated by sonication[14,18] during dissolution and several freeze-thaw cycles), used to prepare the mix in which HA was hydrolyzed. Lanes 5−9 contain the samples taken during HA hydrolysis at 2.17, 3.25, 4.17, 5.30, and 23.25 h, after the beginning of the acidic hydrolysis, showing

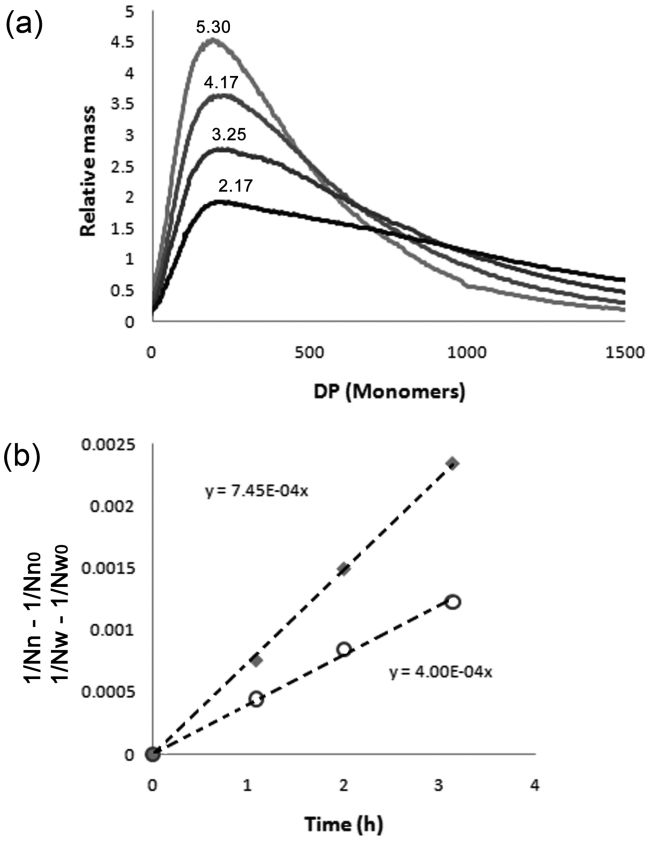

Figure 4. (a) MD at sampling times 2.17, 3.25, 4.17, and 5.30 h, with molecular mass populations on the ordinate and relative mass in the populations on the abscissa. MD was determined up to M = 3300 but depicted only up to 1500. (b) Kinetic plot of $1/N_n - 1/N_{n(0)}$ versus time (rhombi) and $1/N_w - 1/N_{w(0)}$ versus time (circles). The dashed lines correspond to a linear fit.

a progressive shift toward the lower end of the gel, indicative of a progressive reduction of molecular weights.

From the optical density profiles, full MDs, up to 33612 disaccharide long chains, were calculated according to the method described in the Supporting Information. For the MD at 2.17 h, used as input in the model, less than 0.5% of the total mass was in fractions >8000 disaccharides. In Figure 4a, MDs of sample times 2.17 to 5.30 h (agarose gel lanes 5−8) are, for reasons of clarity, depicted up to M of only 1500 disaccharides. Supporting Information, Figure 5S also gives MD at 0 h and at 23.25 h, which were not included in Figure 4a because (1) between 0 and 2.17 h there was a lag time due to warming up of the HA mix in the oven and (2) MD at 23.25 h contains short fragments of a few to a few hundred of disaccharide units, for which diffusion starts to play a major role, causing the peak to broaden and the front of the peak to extend further than what should be expected based on just electrophoresis (as can be seen in Supporting Information, Figure 5S as the MD having a value >0 at M = 0).

3.3. Determination of the Scission Rate Constant. Figure 4a shows the MD evolution upon degradation time. From these MD data, N_n and an N_w were obtained, which were both plotted reciprocally as a function of time, yielding a kinetic plot (Figure 4b). The kinetic plots are linear, which is typical for random degradation.[5,19,20] From the slopes we obtained k_h values of 7.45×10^{-4} (h^{-1}) and 8.00×10^{-4} (h^{-1}) for the N_w and N_n data, respectively. These k_h values are in the range of what is to be expected according to data from similar HA degradation presented by Tømmeraas et al.[19] It is important to realize that Tømmeraas' results have to be (re)interpreted with some care. First, the k_h values listed by Tømmeraas et al. are in fact k'_h values (in units $Da^{-1} \cdot h^{-1}$) derived from kinetic plots with M_w expressed in the unit (Da) on the abscissa (eq 1). A proper k_h, in the units (h^{-1}) should be derived from a kinetic plot in which N_w or N_n are expressed as dimensionless degrees of polymerization. The difference between true k_h and k'_h as reported by Tømmeraas (without writing the prime) is just the molar mass of a disaccharide monomer unit. Furthermore, the M_w-derived k_h is in fact *twice* the slope in the kinetic plot, while Tømmeraas et al., calculated k'_h as *half* the slope instead. From these k'_h values, Tømmeraas draws Arrhenius plots and calculates activation energies. It is important to note that the units in the kinetic plot and the wrongly applied factor of 2 do not affect the slope in an Arrhenius plot, of ln k_h vs $1/T$, but only the absolute values obtained for k'_h. As a result, there is no consequence for the calculations of the (slope-derived) activation energy. We recalculated the rate constant using the data of Tømmeraas et al., using the molar mass of the disaccharide excluding sodium counterions (401 g/mol) and taking into a account the correction factor of 4 (so $k_h = k_h$(Tømmeraas) × 4 × 401), and find $k_h = 1.6 \times 10^{-4}$ (h^{-1}) at 40 °C and 1.6×10^{-3} (h^{-1}) at 60 °C for 0.1 M HCl. Our value of 7.45×10^{-4} (h^{-1}) at 50 °C and 0.1 M HCl is well in line with the data of Tømmeraas et al.

To our surprise, the difference between the N_w-derived and N_n-derived k_h values is somewhat larger than the difference between the two simulated hypothetical cases shown in Figure 2 (7% vs 4%). This discrepancy can be related to the MD at 2.17 h (Figure 4a), since the $MD_{(0)}$ is the determining factor for the N_w vs N_n deviation. At first glance, the MD at 2.17 h (Figure 4a) looks Kuhn-like. However, when examining the distribution more carefully, we find a maximum at approx 200 disaccharides and a weak shoulder at approximately 700 disaccharides. Consequently, the initial N_w/N_n ratio is not 2 but 2.9 and converged toward 2 during the degradation process. At 3.25 h (Figure 4a) the development of these peaks can be observed more clearly as the shoulder at 700 disaccharides has shifted to around 400 disaccharides, while the peak of small fragments has only shifted only slightly to the left.

3.4. Simulations of Degradation of an Experimental Initial Distribution. It would be interesting to see whether a simulation of the degradation using MD at 2.17 h as $MD_{(0)}$ and experimentally determined values for k_h result in the same deviation in the N_w-derived k_h as observed experimentally. To this end, the measured initial $MD_{(0)}$ (in this case at 2.17 h) was discretized, with the size spacing corresponding to a disaccharide unit (Supporting Information) and used as the starting condition of the simulation. In addition, the experimentally determined values for the N_w-derived and N_n-derived k_h were used. Figure 5 shows overlays of experimental MDs (gray solid lines as in Figure 4a) and the simulated ones (dashed lines) for N_n-derived $k_h = 7.45 \times 10^{-4}$ h^{-1} (Figure 5a) and N_w-derived $k_h = 8.00 \times 10^{-4}$ h^{-1} (Figure 5b). From each simulated MD (dashed line), N_n and N_w were calculated and kinetic plots analogous to Figure 4b were made. Figure 5a shows that the model is in line with the experimental data in terms of the slopes to and from the peak and the position of the top of the peak. In Figure 5b, the top of the peak appears to match better because the peak height matches better. However, the slopes to and from the peak match not as

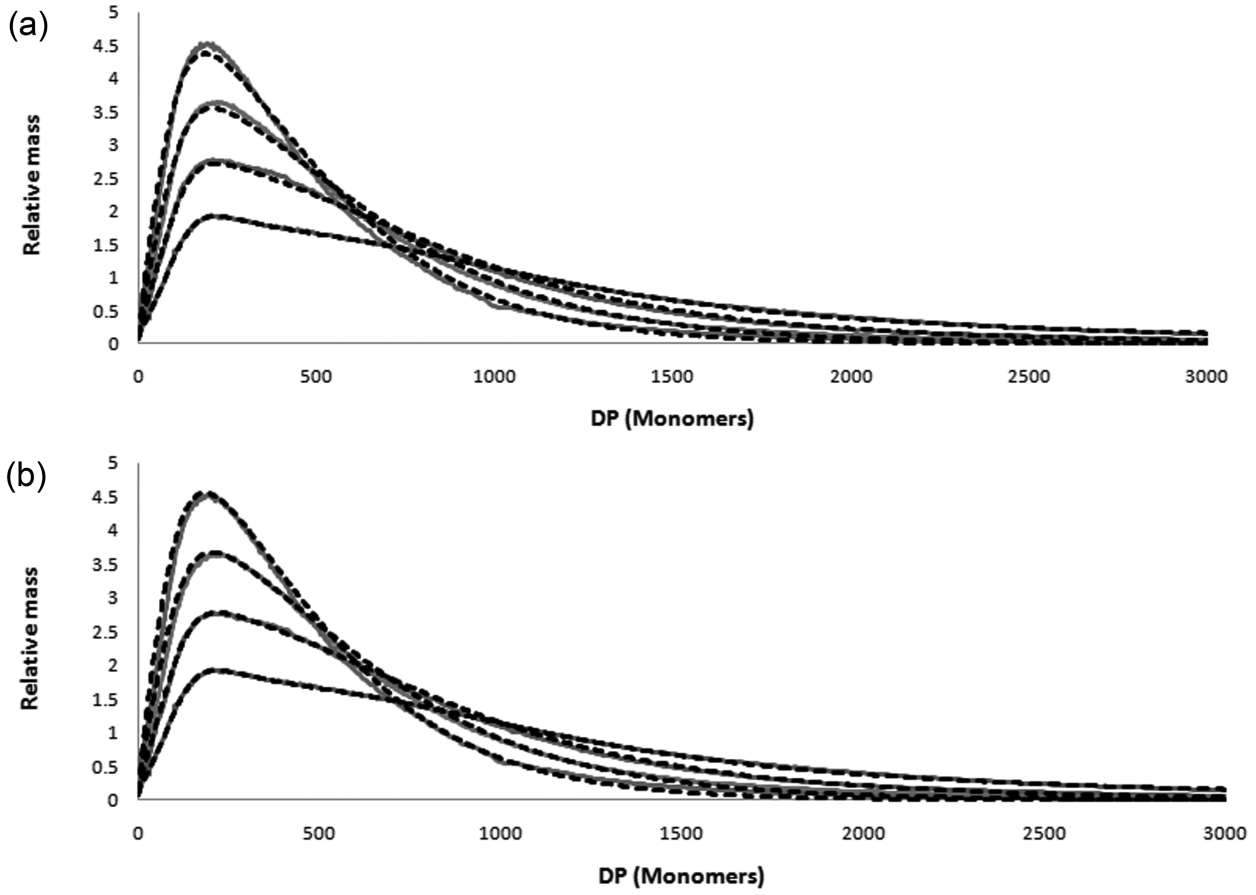

Figure 5. Overlay of measured MD evolution and predicted MD evolution for sampling times 2.17 h, 3.25 h, 4.17 h, and 5.30 h with mass populations on the ordinate and relative mass in the populations on the abscissa. Gray solid lines are the measured MD as in Figure 4a and dashed lines are the simulated MDs: (a) k_h =7.45 × 10^{-4} h^{-1}; (b) k_h =8.00 × 10^{-4} h^{-1}.

good as in Figure 5a and the predicted position of the top of the peak is at lower M compared to the experimental data.

An input k_h of 7.45 × 10^{-4} h^{-1} was used to generate the simulated part of Figure 5a. Subsequently a simulated k_h of 7.43 × 10^{-4} h^{-1} and 8.84 × 10^{-4} h^{-1} was derived from the simulated $N_{n(t)}$ and $N_{w(t)}$, respectively. This shows again internal consistency of the model, accuracy of k_h determined via N_n and a k_h determined from N_w that is higher than the input value just like for Figures 2f and 4b. When using k_h = 8.00 × 10^{-4} h^{-1} as input (Figure 5b), simulating MDs and calculating simulated k_h from N_n and N_w gave k_h values of k_h = 7.97 × 10^{-4} h^{-1}, and k_h = 9.46 × 10^{-4} h^{-1} respectively, the highest being out of range of our experimental results, showing that using N_w to determine k_h in this case is unreliable. All in all, using the N_n-derived k_h as input appears to reproduce the experimental MD evolution during hydrolysis more accurately than using the N_w-derived k_h.

The simulated difference between N_w-derived and N_n-derived k_h is in both cases 19%, which is larger than the 7% difference found for the measured data. That the actual measurement appears more accurate may just be due to experimental inaccuracy in the points of the kinetic plot. This means that using N_w instead of N_n to determine k_h can realistically lead to errors in the order of 20%, especially when starting with $MD_{(0)}$ like the one for MD at 2.17 h.

3.5. Reducing Sugar Essay Determination of k_h. We determined k_h independently using the dinitrosalicylic acid (DNS) assay for reducing sugars.[22] To calibrate the DNS assay we initially used serial dilutions of monomeric GlcNac. We found that, the later a sample was taken during HA degradation, the higher the reducing sugar concentration (Figure 6a). Because bond scission follows first-order kinetics, a monoexponential approach of the reducing end concentration toward a final plateau should be expected. Determining the initial rate of reducing end formation (slope of a linear approximation of the curve in Figure 6 during the first 30 h) divided by the concentration of bonds that are available for cleavage will directly give k_h.

The rate determined from Figure 6a is k_h = 4.1 × 10^{-3} h^{-1}, which is not consistent with the measurements and model above, implying that either our MD study and model is wrong, or that the calibration of the reducing end concentration is not correct. A previous study describes that monomeric reducing sugars develop much less color in the DNS assay than the same reducing sugars on the end of a long chain, and that the effect reaches a plateau at a chain length >10 monomers.[24] Therefore, we investigated the dependency of extinction coefficient of a terminal reducing GlcNac in the DNS assay as a function of HA chain length (Figure 6b). It appeared that at a chain length of 10 monosaccharides, the extinction coefficient was 5 times higher than that of mono-GlcNac. Consequently, k_h determined from Figure 6a is 5 times too high. However, a careful look at the earlier described data[24] shows that the extinction coefficient increases with another ~16% between DP = 14 and DP = 46

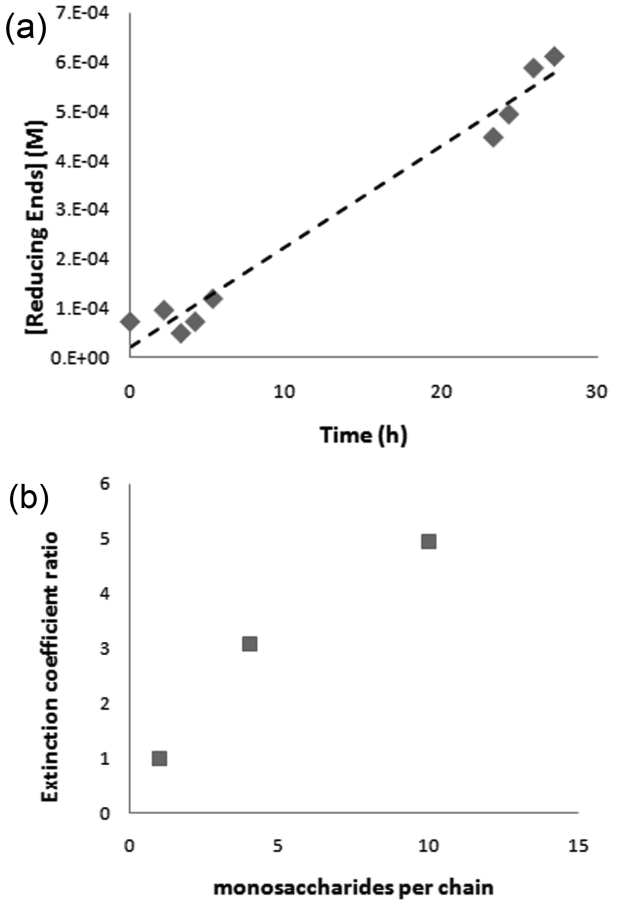

Figure 6. (a) Apparent reducing sugar concentration (rhombi) in time for HA degrading at pH = 1.1 and T = 50 °C, as determined with DNS reducing sugar assay and calibrated with serial dilutions of a monomeric GlcNac standard. The slope of the dashed line gives the apparent production rate of reducing ends, hence the apparent bond cleavage rate. (b) Ratio of extinction coefficient in DNS reducing sugar essay between monomeric GlcNac, and GlcNac at the end of a 4 and a 10 monosaccharide long HA chain.

monosaccharides. Unavailability of monodisperse HA samples >10 monosaccharides disallowed us to precisely determine the plateau value. Still, taking a correction factor of 4.95 as the lower limit and (1.16 × 4.95=) 5.74 as the upper limit we eventually obtain: $7.2 \times 10^{-4} < k_h < 8.3 \times 10^{-4}$ from the reducing sugar essay for HA degradation at 50 °C and pH 1.1. The k_h obtained from N_n and N_w now both fall exactly within this range.

The hypothetical reducing end concentration after total conversion, calculated by dividing the weight concentration by the molar mass of a disaccharide (including sodium counterion) would lead to (2/401=) 5 mM of reducing ends. We recalculated the final concentration of reducing ends in Figure 6a to be 0.12 mM which is only 2.4% of the total conversion concentration, justifying the linear approximation in Figure 6a of the monoexponential curve during the first 30 h from which the slope was taken to obtain k_h.

4. CONCLUSIONS

Our results and analysis confirm that HA hydrolysis under acidic conditions follows random scission. The presented model in combination with a correctly determined k_h (7.45×10^{-4} (h^{-1})) for practical working conditions (0.1 M HCl at 50 °C) can facilitate the industrial use of hydrolysis in the preparation of HA MDs for medical and cosmetic purposes. The presented numerical model allows for the analysis of the degradation as well as prediction of MD evolution of arbitrary initial distributions.

From the simulated scenarios (Figure 2, parts a and d), it is clear that it is more precise to calculate k_h from an N_n-based kinetic plot than from an N_w-based kinetic plot, though the N_w-derived k_h deviated no more than 5% from the k_h input in these hypothetical cases. The N_n-based kinetic plot is intrinsically linear, while the N_w-based kinetic plot is slightly curved and straightens out at later times as the N_w/N_n ratio approaches 2. Therefore, including early points from the linear fit in the N_w kinetic plot leads to an error in k_h, and the method for determining k_h through N_w is mainly accurate for large degrees of degradation. The difference between the experimental and theoretical N_n-derived and N_w-derived k_h (7% vs 19%) could be explained by experimental inaccuracy, indicating that our measured k_h may vary by as much as (19% − 7%=) 12% from the actual k_h value, but judging from the reducing-end study, it is probably less. Regarding the use of N_w it is clear that in principle the N_w-derived k_h can only be used, once a Kuhn distribution has established itself. This means that in an Ekenstam plot, points obtained early during a degradation reaction may have to be ignored. In case the N_n-based kinetic plot is used, one does not have to wait until a Kuhn distribution has established itself, allowing for a quicker determination of k_h. On the basis of our findings we conclude that the use of N_n data for the determination of k_h is more correct and faster as compared to the commonly used N_w-based approach.

5. EXPERIMENTAL SECTION

Calculations. All calculations were performed in MS Excel. A size population model for random scission of a linear polymer was built to describe the random degradation of HA under acidic conditions. The model and calculations are elaborated upon in section 2 and in the Supporting Information.

Chemicals. Hyaluronic acid sodium salt from *S. zooepidemicus* was purchased from Sigma-Aldrich Chemie B.V. (Zwijndrecht, The Netherlands). According to the specs of the supplier the HA is 1−4 MDa in weight. According to our gel-electrophoresis determination the HA batch has a M_w and M_n of 1.4 MDa and 0.3 MDa, respectively (including Na counterion). Phosphate salts (for buffers), 1 M HCl, NaOH pellets, ethanol, stainsall, 5,3-dinitrosalicylic acid, Rochelle salts, phenol, and sodium metabisulfite were also purchased from Sigma-Aldrich Chemie B.V. (Zwijndrecht, The Netherlands). HA molecular mass markers: SelectHA HiLadder and MegaHA ladder as well as monodisperse sample of 4 monosaccharide long HA chains: OligoHA4 and monodisperse sample of 10 monosaccharide long HA chains OligoHA10 were purchased from Hyalose LLC (Oklahoma City USA). For dilutions and sample preparation, Milli-Q water from a Millipore (Amsterdam, The Netherlands) AFS D3 system was used.

Hyaluronan Degradation for Sampling. A 5 g/L stock solution was made in MQ water by allowing HA to dissolve undisturbed overnight at 4 °C. Another 5 g/L HA stock solution was prepared by adding water to the HA powder, sonifying for 2 h in a Cole Parmer ultrasonic cleaning bath, leaving the solution for another 2 h and finally freezing the solution at −20 °C. This latter HA stock, MQ, and 1 M HCl were mixed (in this order) to final concentrations of 2 g/L HA and 0.1 M HCl, and placed in a glass vial in an oven at 50 °C. During degradation, samples of 750 μL were taken in which the degradation reaction was

immediately stopped by adding 75 μL neutralization buffer, quick mixing, and cooling on ice. Neutralization buffer was prepared earlier by mixing 2M NaOH with 400 mM phosphate buffer pH 7 in a 1:1 ratio. After neutralization, samples were stored at −20 °C.

HA Preparation for Agarose Gel Electrophoresis. HA molecular mass (MW) markers were dissolved according to specifications. The HA samples were first diluted by taking, 19.5 μL of neutralized HA sample and adding 70.5 μL of MQ. Molecular mass markers and samples were finally prepared for loading on gel by taking 5 μL of the MW marker solution or diluted sample and adding 3 μL of 2 M sucrose in Tris-acetate-EDTA (TAE) and 10 μL of MQ.

Agarosegel Electrophoresis. A 0.5% agarose gel (molecular biology grade) in TAE buffer was cast with a 20 tooth well-forming comb and run in TAE buffer in a Biorad Wide Mini-Sub Cell. MW markers and samples were loaded. Every second well was kept empty. The gel was run at 20 V for 15 min, then at 40 V for 1.5 h, after which the TAE buffer was replaced by fresh buffer. The gel was then run for another 1.5 h, after which the gel was stained.

HA Staining in Agarose Gel. Stainsall staining solution was prepared in the dark by dissolving 0.05 g/L Stainsall in 50% ethanol. After electrophoresis, the agarose gel was stained overnight in staining solution in a plastic box wrapped in aluminum foil on a shaker. The staining solution was removed and the gel was destained in 10% ethanol in the dark for a day, during which the 10% ethanol was replaced twice. After destaining, the gel was bleached for 8 min on a UV transilluminator.

Densitometry. The gel was scanned using a Biorad GS-800 calibrated densitometer and the image analyzed with the Quantity One software package. In Quantity One, lanes were defined and the relative position on the gel was defined from 0 to 1: 0 being just under the well and 1 close to the bottom of the gel. Optical density profiles (ODP) (optical density as a function of relative position) for every lane on the gel were exported as .txt files and imported into MS Excel. For each sample containing lane, the background was determined by averaging the ODP of the two empty adjacent lanes. This background ODP was then subtracted from the ODP of the sample containing lane, yielding a background corrected ODP (Supporting Information). As described in the Supporting Information, molecular mass (MW) markers enabled the conversion of ODP to molecular mass distribution (MD).

DNS Reducing Sugar Assay. DNS reducing sugar assay was used as essentially described by Miller.[22] DNS reagent is sensitive to both oxygen and light, so to prepare DNS reagent, first 250 mL of MQ was boiled and then flushed with argon to replace oxygen, then while still warm but <50 °C, 231 mL was transferred to a brown (light blocking) glass bottle on a magnetic stirrer, and the following was dissolved in order: 1.73 g of 5,3-dinitrosalicylic acid, 3.235 g of NaOH, 50 g of Rochelle Salts, 1.33 g of phenol, 1.36 g of sodium metabisulfite. The headspace was then again flushed with argon. The DNS reagent was stored at 4 °C. Because the DNS reagent can denature in time, a serial of reducing sugar standards for calibration have to be included with every batch of samples. For calibration of the DNS assay, a serial dilution of GlcNac was included with every batch of samples. Samples had neutralization buffer added, so to directly compare sugar concentrations in samples and standards, 275 μL sample was taken for analysis, while for standard 250 μL was taken and 25 μL MQ added before analysis. To increase sensitivity for low sugar concentrations, an aliquot of DNS reagent was premixed with 6.4 g/L GlcNac in a volume ratio of 20:1. Of this premix, 525 μL was added to each sample and each standard contained in an Eppendorf tube. Samples and standards were then heated for 5 min at 95 °C in a stirred water bath and cooled quickly in an other water bath at room temperature. Finally, the boiled samples and standards were diluted 10 times and extinction was read out at 540 nm on a Shimadzu UV-1800 spectrophotometer. All samples were compared to GlcNac monosaccharide standard serial dilutions. OligoHA4 and oligoHA10 standards were measured together with the GlcNac standard, providing a conversion factor between the extinction coefficients of mono-GlcNac and GlcNac at the end of a HA chain.

■ ASSOCIATED CONTENT

Supporting Information. Implementation of the model and calculations in MS Excel, densitometry, and *M* calibration curves to calculate final measured MDs. This material is available free of charge via the Internet at http://pubs.acs.org.

■ AUTHOR INFORMATION

Corresponding Author

*E-mail: a.a.martens@tudelft.nl (A.A.M.); n.a.m.besseling@tudelft.nl (N.A.M.B.).

■ ACKNOWLEDGMENT

We thank Professor Mary K. Cowman (NYU-Poly), for providing the protocols for hyaluronan electrophoresis, staining and densitometry and Mr. E. Kusadasi and Mr. S. Lawant for performing preliminary experiments. LCPMdS is financially supported by a VENI grant from The Netherlands Organization for Scientific Research (NWO).

■ REFERENCES

(1) Kuhn, W. *Ber. Dtsch. Chem. Ges.* **1930**, *63*, 1503–1509.
(2) Tanford, C. *Physical Chemistry of Macromolecules*; Wiley: 1961.
(3) Montroll, E. W.; Simha, R. *J. Chem. Phys.* **1940**, *8* (9), 721–727.
(4) Simha, R. *J. Appl. Phys.* **1941**, *12* (7), 569–578.
(5) Emsley, A. M.; Heywood, R. J. *Polym. Degrad. Stab.* **1995**, *49* (1), 145–149.
(6) Staggs, J. E. J. *Polymer* **2007**, *48* (13), 3868–3876.
(7) Stern, R.; Asari, A. A.; Sugahara, K. N. *Eur. J. Cell Biol.* **2006**, *85* (8), 699–715.
(8) Laurent, T. C.; Fraser, J. R. E. *FASEB J.* **1992**, *6* (7), 2397–2404.
(9) Lesley, J.; Hyman, R.; Kincade, P. W. *Adv. Immunol.* **1993**, *54*, 271–335.
(10) Toole, B. P. *Semin. Cell Dev. Biol.* **2001**, *12* (2), 79–87.
(11) Rinaudo, M. *Polym. Int.* **2008**, *57* (3), 397–430.
(12) Falcone, S. J.; Palmeri, D.; Berg, R. A. *Polysaccharides Drug Delivery Pharm. Appl.* **2006**, *934*, 155–174.
(13) Kogan, G.; Soltés, L.; Stern, R.; Gemeiner, P. *Biotechnol. Lett.* **2007**, *29* (1), 17–25.
(14) Stern, R.; Kogan, G.; Jedrzejas, M. J.; Šoltés, L. *Biotechnol. Adv.* **2007**, *25* (6), 537–557.
(15) Kooy, F. K.; Ma, M.; Beeftink, H. H.; Eggink, G.; Tramper, J.; Boeriu, C. G. *Anal. Biochem.* **2009**, *384* (2), 329–336.
(16) Yoshida, M.; Itano, N.; Yamada, Y.; Kimata, K. *J. Biol. Chem.* **2000**, *275* (1), 497–506.
(17) Shiedlin, A.; Bigelow, R.; Christopher, W.; Arbabi, S.; Yang, L.; Maier, R. V.; Wainwright, N.; Childs, A.; Miller, R. J. *Biomacromolecules* **2004**, *5* (6), 2122–2127.
(18) Kubo, K.; Nakamura, T.; Takagaki, K.; Yoshida, Y.; Endo, M. *Glycoconjugate J.* **1993**, *10* (6), 435–439.
(19) Tømmeraas, K.; Melander, C. *Biomacromolecules* **2008**, *9* (6), 1535–1540.
(20) Hjerde, T.; Smidsrød, O.; Christensen, B. E. *Carbohydr. Res.* **1996**, *288*, 175–187.
(21) Lee, H. G.; Cowman, M. K. *Anal. Biochem.* **1994**, *219* (2), 278–287.
(22) Miller, G. L. *Anal. Chem.* **1959**, *31* (3), 426–428.
(23) Inoue, Y.; Nagasawa, K. *Carbohydr. Res.* **1985**, *141* (1), 99–110.
(24) Sengupta, S.; Jana, M. L.; Sengupta, D.; Naskar, A. K. *Appl. Microbiol. Biotechnol.* **2000**, *53* (6), 732–735.